

# Detection and Maintenance of Switch Machines based on Image Technology

Manfei Chen<sup>1</sup>, Jiakuan Li<sup>2</sup>, Zhenhua Long<sup>3</sup>, Kaikai Hu<sup>3</sup>, Xingxing Ma<sup>1</sup>,  
Haojia Zhang<sup>1</sup>, and Yu Jia<sup>1</sup>

<sup>1</sup> Baoji Electric Depot of China Railway Xi'an Bureau Group Co., Ltd., Xi'an, Shaanxi, China

<sup>2</sup> Xi'an Communication Section of China Railway Xi'an Bureau Group Co., Ltd., Xi'an, Shaanxi, China

<sup>3</sup> Yan'an Operation and Maintenance Section of China Railway Xi'an Bureau Group Co., Ltd., Xi'an, Shaanxi, China

---

## Abstract

**In response to the issues of incomplete inspection resulting from manual periodic checks during the maintenance of railway switches, this paper proposes a method for detecting and maintaining railway switches based on image technology. This method utilizes multiple images with varying pixel densities to perform multi-view three-dimensional reconstruction, obtaining sparse point clouds, dense point clouds, mesh models, and texture mapping models of the railway switches. The three-dimensional information of the railway switches, such as the dynamic and static contact points, is derived from the dense point cloud, while the reconstructed texture mapping model allows for intuitive observation of the status of various parts of the switches. Experimental results show that the average deviation of the contact depth of the dynamic contact points is 0.1438mm, with an average error of 2.58%. Therefore, this algorithm can effectively detect the dynamic and static contact point status of railway switches.**

## Keywords

**Railway Track Bed; Switches; Theoretical Analysis; Image Processing.**

---

## 1. Introduction

In the wake of urban expansion and rapid economic growth, railways have emerged as pivotal modes for both passenger and freight transportation. However, as the density of railway traffic increases, the burden of maintaining railway equipment escalates. Consequently, the application of artificial intelligence (AI) technologies to replace manual inspection and monitoring tasks becomes an inevitable trend.

Among railway infrastructure failures, incidents involving railway switches constitute a significant portion. These switches, crucial for diverting railway tracks, locking them, and indicating the position of track points, hold paramount importance. Any malfunction in these switch machines during operation can lead to trains being unable to navigate properly, potentially resulting in accidents. Thus, the pressing challenge lies in devising more intelligent and efficient methods to inspect and maintain switch machines, enabling precise, reliable, and comprehensive predictive warnings.

In recent years, experts have proposed various monitoring methods, mainly focusing on indicators such as voltage, current, action time, and gap detection[1]-[2] for switch machines. He Hui[3] et al. (2023) introduced a diagnostic method based on DCNN SVM for switches, utilizing the similarity between action curves and standard curves to distinguish between normal and abnormal switch

operations. This method employs deep learning to compute image features, coupled with model training using a training set, ultimately achieving real-time diagnosis of switch failures. However, given that switch machines are outdoor equipment operating in complex field environments, the aforementioned method, while capable of issuing alerts for certain issues, fails to provide intuitive and accurate determinations of switch operational statuses, leaving numerous undetectable problems unresolved.

Amidst the rapid advancement of sensors, the innovation in utilizing image processing techniques for detecting switch machine statuses continues to evolve. Du Sen[4] et al. (2023) proposed a pixel-counting-based edge detection algorithm that integrates the Canny operator and dynamic thresholding. Through experimentation, the accuracy improved by 4.83% compared to the original algorithm, exhibiting robustness against environmental noise. Meanwhile, Liu Yunting[5] et al. (2022) introduced a fast fuzzy clustering algorithm based on superpixels (SFFCM) for precise segmentation of gap images. Although image processing techniques are widely applied in gap detection, manual intervention remains essential for the routine maintenance of switch machines. Thus, researchers have begun exploring the utilization of image processing techniques to detect dynamic and static contact points of switch machines. Shi Cong[5] et al. (2020) proposed an image processing-based technique for detecting the status of switch machine dynamic and static contact points, incorporating deep learning methods for extensive machine training, thereby achieving real-time detection of dynamic and static contact points. Additionally, Hu Xiaoxi[7] et al. (2023) introduced an object detection method based on deep feature matching, effectively resolving geometric dimension data of static contact points, with experimental positioning detection accuracy reaching 85.93% and recall rate reaching 90.63%.

While the aforementioned methods effectively monitor some latent risks, switch machines remain susceptible to various factors and mechanical characteristics, resulting in frequent failures. Currently, manual periodic maintenance remains the approach to effectively mitigate faults. However, manual periodic maintenance faces several issues:

- 1) Traditional manual maintenance of switch machines is time-consuming and labor-intensive due to their large numbers, demanding high skill levels from maintenance personnel. Additionally, the complexity of maintenance procedures may lead to oversight or incomplete inspection steps.
- 2) Discrepancies in the technical proficiency and standardized operation levels among personnel conducting manual on-site maintenance may result in omissions or the absence of data, thereby lacking the basis for subsequent issue investigations or reviews.
- 3) The current methods utilizing image processing for switch machine detection are relatively limited in content and scope when using two-dimensional image detection, thus unable to effectively obtain multiple values.
- 4) With the continuous advancement of railway large-scale, intelligent, and computing power, utilizing intelligent methods for detection is more accurate compared to manual contact measurement schemes and reduces the likelihood of accidental collisions.

In traditional image processing methods, using two-dimensional images for detection may compromise measurement accuracy and completeness due to angles of capture and limited information in single-frame images. Hence, this paper proposes a detection and maintenance method for switch machines based on image technology. It employs multiple images for three-dimensional reconstruction of switch machines to obtain point cloud data[8], thereby inspecting whether the dynamic and static contact points of switch machines meet requirements. Simultaneously, surface reconstruction and texture mapping are used to observe the appearance of screws, gaskets, automatic openers, etc., ensuring proper connection of switch machines. This algorithm effectively enhances detection efficiency and accuracy while retaining two-dimensional and three-dimensional data for subsequent reviews, demonstrating a certain degree of foresight.

## 2. The Structure of the Switch Machine

In the realm of railway infrastructure, the pivotal component known as the switch machine stands as the nucleus, serving as a vital electrical signaling apparatus. Taking the ZD6 series electric switch machine as a prime example, a schematic overview of the switch machine is illustrated in Figure 1.

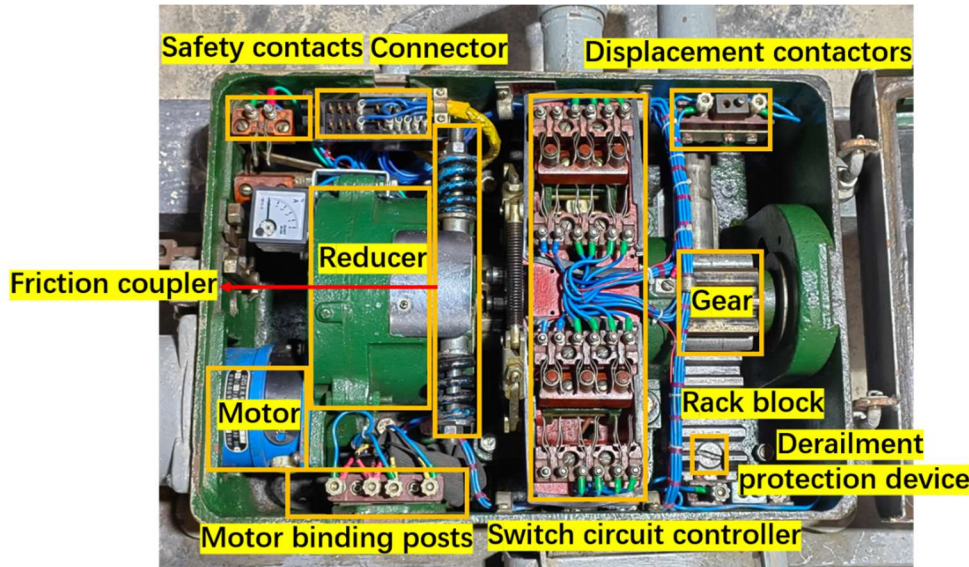


Figure 1. Schematic overview of the switch machine

The ZD6 series switch machine primarily comprises an electric motor, a reducer, a friction coupler, a conversion locking device, an indicating rod, a switch circuit controller, and a derailment protection device, among other components. The signal tower provides control power to the electric motor, which, in turn, imparts motion to the switch rails for directional switching. The reducer functions to reduce the rotational speed of the electric motor. Meanwhile, the friction coupler serves to connect the main shaft and the reducer, aimed at absorbing rotational inertia to safeguard the motor. The switch circuit controller, consisting of rack blocks, locking gears, and actuating rods, facilitates the internal locking process by converting rotary motion to linear motion, thereby driving the tip displacement to achieve internal locking. The indicating rod, comprising front and rear indicating rods and inspection blocks, engages with the check block upon tight adherence of the switch rails, triggering the action of the automatic opener. The automatic opener discerns whether the switch rails are in the designated or reverse position. Instances of malfunction in the automatic opener, such as excessive friction on the locking column leading to jamming, may result in the absence of rail indication, necessitating periodic inspections. Lastly, the derailment protection device severs the circuit upon derailment, thereby safeguarding other mechanical components.

## 3. Overall Design

Considering the comprehensive design for detecting and maintaining switch machines based on image processing, the overall framework encompasses image acquisition, image preprocessing, 2D image detection, and 3D model detection. However, given the existing video detection systems for gap detection in ZD6 models, the additional step of 2D monitoring inspection is unnecessary.

Maintenance personnel utilize smartphones to capture images of switch machines, which are then uploaded for preprocessing by the backend server upon image acquisition. Subsequently, sparse point cloud reconstruction, dense point cloud reconstruction, surface reconstruction, texture mapping, and other procedures are performed based on the images to ultimately generate a three-dimensional model. This model is then utilized to analyze the existence of anomalies in switch machine dynamic and static contact points, connections, appearance, etc. The detection data is finally relayed back to

maintenance personnel, providing effective data support. The schematic overview of the overall design process is depicted in Figure 2.

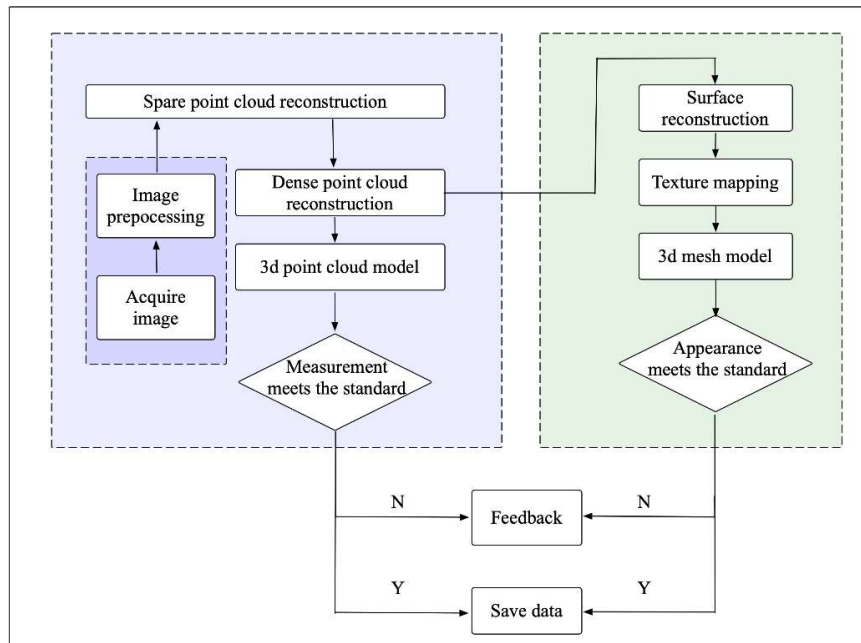


Figure 2. Overall design flow chart

### 3.1 Image Acquisition and Processing

The quality of captured images significantly influences subsequent processing stages. Thus, during image acquisition of switch machines, the following aspects should be considered: (1) Efforts should be made to ensure that the switch machine occupies a significant portion of the image pixels to minimize unnecessary scene interference, thereby reducing the occurrence of irrelevant feature points during subsequent feature matching, which may result in diminished relevant information. (2) Image-based three-dimensional reconstruction techniques rely on multiple images to restore three-dimensional structures. Therefore, there should be a certain overlap or common viewing area between consecutive images to ensure successful feature point matching and subsequent three-dimensional information reconstruction. (3) Image clarity should be maintained during image capture, with efforts made to minimize blurring caused by factors such as shaking. It is noteworthy that in nighttime environments, if necessary, the flash should be activated to ensure image effectiveness. Given that image-based three-dimensional reconstruction algorithms are computationally intensive, preprocessing of the images is required post-acquisition. This involves filtering out blurry, overlapping, and overly bright images, while adjusting the threshold for pixel size-based filtering.

### 3.2 Image-Based Three-Dimensional Reconstruction

The process of obtaining models through image-based three-dimensional reconstruction primarily consists of four parts: sparse point cloud reconstruction, dense point cloud reconstruction, mesh model reconstruction, and texture mapping. Structure from Motion [9, 10](SFM) is a technique used to estimate three-dimensional structures from a series of unordered two-dimensional images containing visual motion information and to optimize the estimation of camera parameters. As depicted in Figure 3, the process flowchart for sparse point cloud reconstruction involves using an incremental SFM algorithm to select suitable image matching pairs from the image set, followed by the incremental addition of other images to continuously calculate and obtain the sparse point cloud model. Given that this algorithm requires pairwise image matching, it necessitates a sufficiently wide baseline and an adequate number of matching points to ensure that adjacent images have common viewing areas.

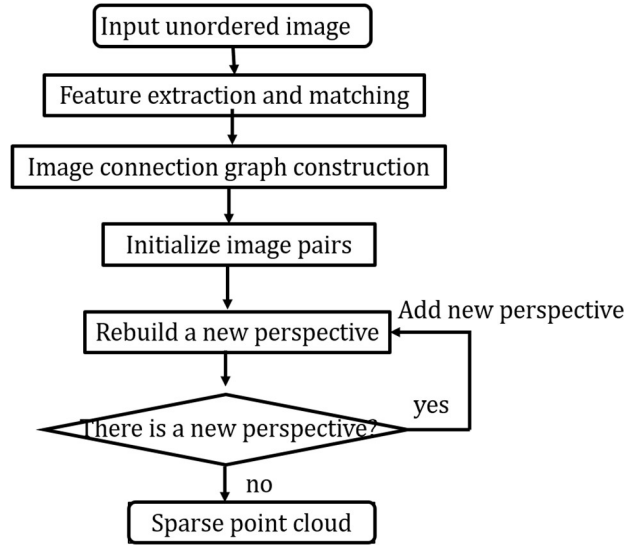


**Figure 3.** Sparse point cloud reconstruction flow chart

After obtaining the sparse point cloud model, it's evident that further reconstruction into a complete three-dimensional model is necessary. Hence, employing a multi-view stereo vision algorithm for dense point cloud reconstruction becomes imperative. In this regard, the Depth Image Fusion-based Multi-View Stereo (MVS) algorithm is chosen for its capabilities in stereo pair selection, depth map computation and optimization, as well as depth image fusion. The ultimate objective is to achieve a reconstructed three-dimensional point cloud model exhibiting robustness and practicality.

When selecting stereo pairs, it is essential to input images along with their corresponding camera intrinsic and extrinsic parameters initially. Subsequently, ineffective, uncalibrated, or discarded images are filtered out. Then, all useful neighboring frames are selected for each reference image. A suitable selection strategy significantly enhances the reconstruction effectiveness, making this step crucial. Finally, utilizing Markov Random Field (MRF) optimization, a global best neighboring view is chosen for each reference image. The strategy for selecting neighboring frames involves factors such as the angle between common viewing points  $f$  in two images  $V$  and  $R$ , denoted as  $\omega_N$  and  $f$ ; the similarity in resolution between two images, represented as  $\omega_S$  and  $f$ ; and the minimum area covered in two images, denoted as  $area$ . The score is calculated as follows:

$$Score(V) = area_R \cdot \sum_{f \in F_V \cap F_R} \omega_N(f) \cdot \omega_S(f) \quad (1)$$

Here,  $area_R$  represents the minimum coverage area of  $f$  in  $R$ , and  $\omega_N(f)$  denotes the angle between  $f$  in two views. This indirectly determines whether the baseline between two views is sufficiently large.

In the previous step, multiple neighboring frames for each image have already been calculated. However, determining the best neighboring frame to provide reliable data for subsequent depth map computation remains a challenge. This problem is addressed using the energy optimization algorithm based on Markov Random Field (MRF).

$$energy(X, Y) = \sum_i UnaryCost(y_i, x_i) + \sum_{j=neighbor(i)} PairwiseCost(x_i, x_j) \quad (2)$$

$Y$  represents the label,  $X$  denotes the node,  $UnaryCost(y_i, x_i)$  is the normalized average score calculated from Formula 1, and  $PairwiseCost(x_i, x_j)$  penalizes cases where labels of two nodes are the same, discouraging identical views between any two images.

In the second step, depth map computation follows the principles of the PatchMatch algorithm, as illustrated in Figure 4. Here,  $C_i$  and  $C_j$  represent the camera centers of the stereo pair,  $P$  denotes a pixel point on  $I_i$ , and a plane is identified on the ray connecting  $C_i$  and  $P$ . This plane minimizes the aggregation cost between the current image  $I_i$  and the neighboring image  $I_j$ , making  $f_2$  the tangent plane for surface reconstruction.

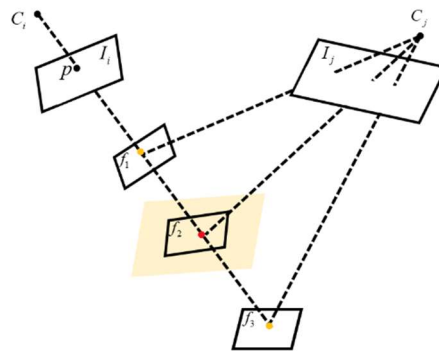


Figure 4. Finding the minimum aggregation plane

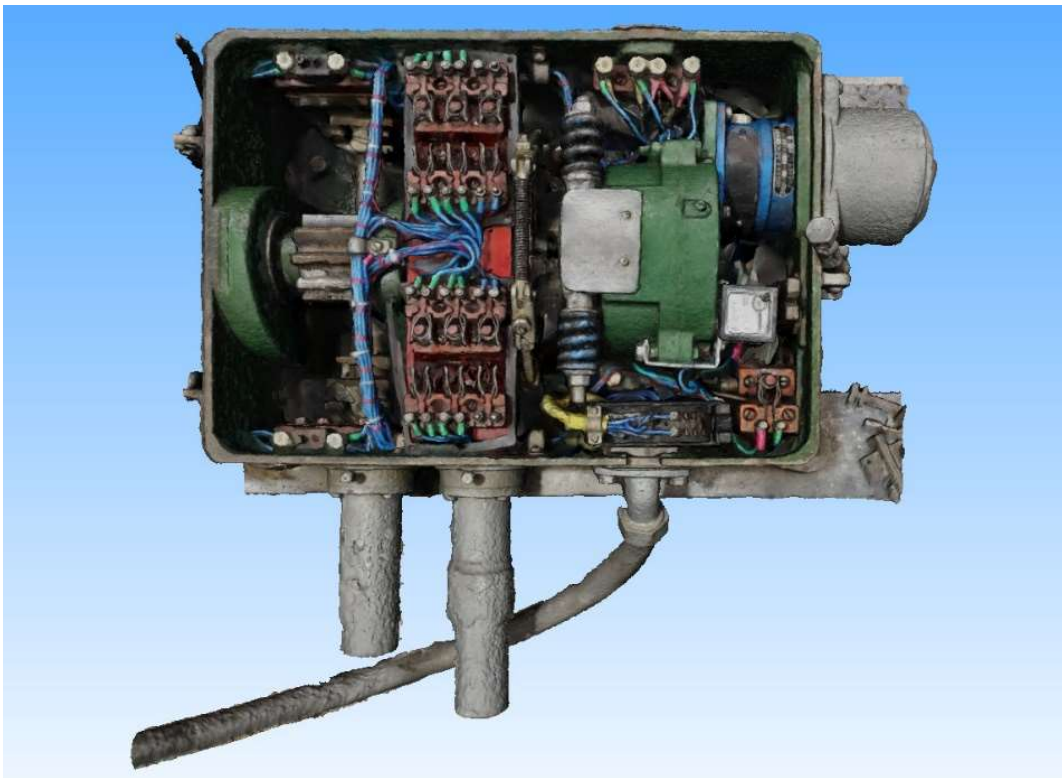
After identifying the plane with the minimum aggregation cost for each pixel in the stereo pair, the initialization of the depth and normals of the tangent plane is conducted. Subsequently, the correct disparity planes from all initial disparity planes are propagated to other pixels within the same disparity plane. This is achieved through iterative spatial propagation and random assignment, aiming to obtain an effective depth map. However, due to depth errors, the original depth map may not be entirely consistent in common regions. Therefore, it is necessary to detect depth consistency, assessing whether the depth of the formula region of an image and its neighborhood is consistent. Any discrepancies are addressed by removing them to ensure a relatively accurate depth map. Finally, a depth map merging operation is performed to obtain a dense 3D point cloud. The resulting point cloud is typically very dense, especially when using high-resolution images.



Figure 5. Dense point cloud reconstruction of switch machine

Upon dense point cloud reconstruction, the switch machine has acquired valid three-dimensional information, as depicted in Figure 5. However, as illustrated in Figure 4, discrete points fail to accurately describe the three-dimensional entity. To address this issue, a mesh reconstruction algorithm is introduced to form a complete three-dimensional model, which is then optimized using the mesh model optimization technique.

Texture mapping, a technique for generating colored texture maps on meshes, involves adding color information to the three-dimensional model. This algorithm maps 2D images onto the 3D model, selecting appropriate views for each triangular face. Additionally, color blending is performed to eliminate color differences in images captured from different viewpoints. The resulting three-dimensional model contains color information, as shown in Figure 5. Compared to the point cloud information, the model reconstructed using mesh reconstruction and texture mapping appears more complete and robust in Figure 6. This allows for better observation of the status of various components.



**Figure 6.** Texture mapping model of switch machine

#### **4. Experiments and Case Analysis**

In this experiment, the ZD6 type turnout machine is used as an example, and ordinary smartphone cameras are employed for image acquisition. To reduce computational load, two sets of images with different pixel sizes, 600800 pixels and 40003000 pixels, are captured. A total of 117 images compose a complete image set for subsequent reconstruction, as depicted in Figure 7. Figure 8 illustrates the schematic diagram of the poses of the turnout machine obtained after sparse point cloud reconstruction from various poses of the turnout machine. Additionally, Figure 8 demonstrates that the sparse point cloud obtained after sparse point cloud reconstruction of the turnout machine is extremely sparse and unable to represent the structural framework of the turnout machine.

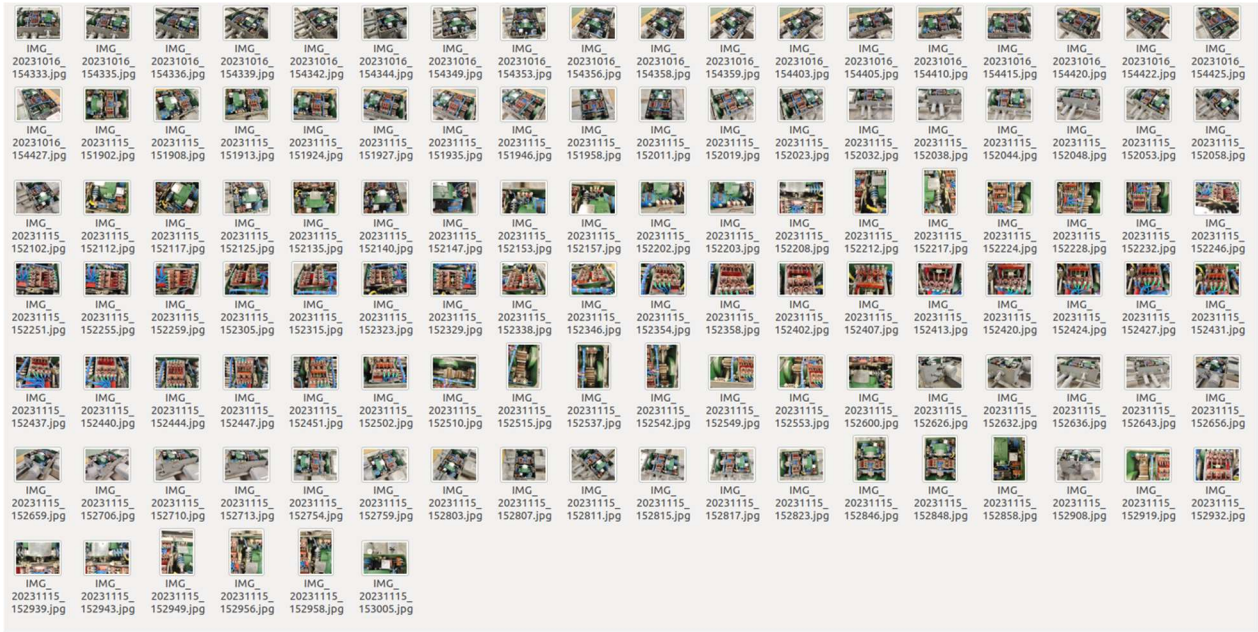


Figure 7. Schematic diagram of image acquisition

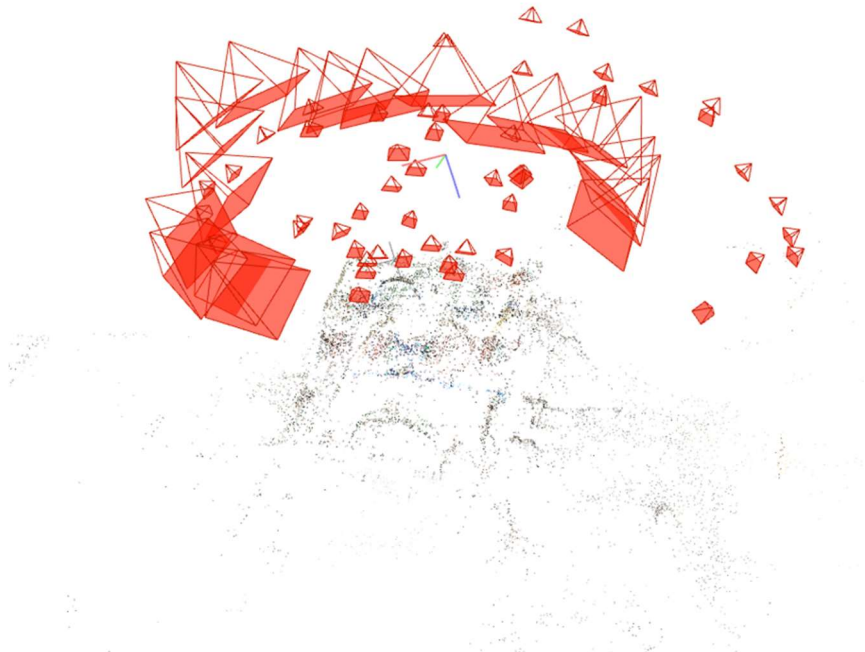
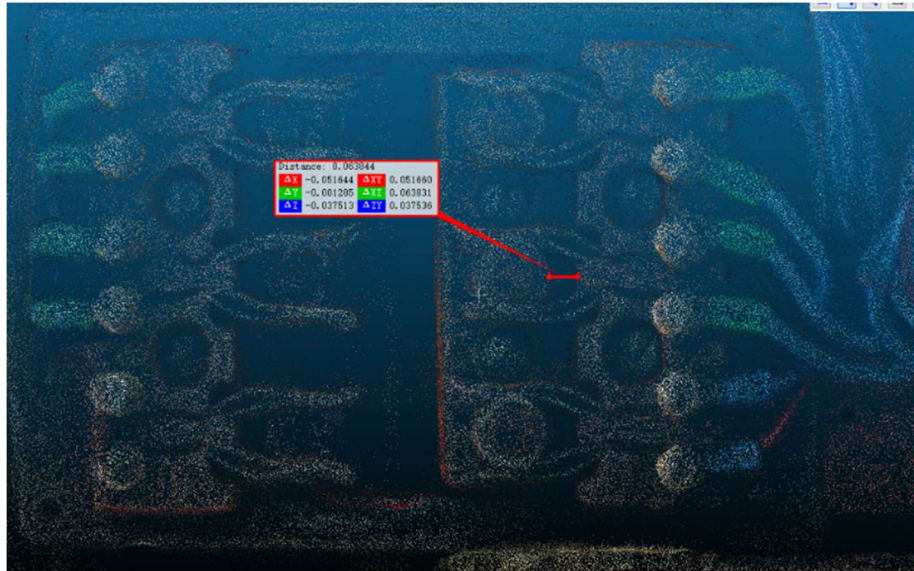


Figure 8. Schematic diagram of switch machine posture

Figure 5 shows the schematic diagram of the dense point cloud reconstructed from the image set. It is evident from the figure that the three-dimensional structure of the turnout machine and the positions of its various components are clearly visible. Since the subsequent mesh reconstruction and optimization rely on the point cloud model in the dense point cloud, measurements based on the dense point cloud model are more accurate. Figure 9 presents a partial schematic diagram of the dense point cloud of the automatic switch opener, which is used for point cloud measurement using CloudCompareStereo software to obtain relative distances.



**Figure 9.** Partial dense point cloud diagram of automatic opening and closing device

After measuring the terminal dimensions of the movable contact point, the contact depth of the movable contact point within the static contact point plate can be calculated to determine if the automatic switch opener meets the standards, with a minimum requirement of not less than 4mm.

Using a micrometer caliper with an accuracy of 0.01mm, the diameters of the six terminals are measured, and the contact depth of each terminal is calculated. A comparison with the measured true values is presented in the table below:

**Table 1.** Contact depth calculation table of terminals Unit: mm

Terminal number	1	2	3	4	5	6
Terminal real value	10.36	9.57	9.51	9.5	9.55	9.54
Terminal relative measurements	0.1134	0.1097	0.125	0.121	0.127	0.095
True value of contact depth	8.77	8.28	8.02	8.28	8.4	8.75
Contact depth solution value	8.678	8.6463	8.0514	8.5527	8.0949	8.513
absolute difference	0.092	0.3663	0.0314	0.2727	0.3051	0.237
Terminal real value	10.36	9.57	9.51	9.5	9.55	9.54

Based on the findings presented in Table 1, the average deviation in the contact depth of the six movable contact points is determined to be 0.1438mm, with individual error values of 1.05%, 4.42%, 0.39%, 3.29%, 3.63%, and 2.7%. The average error rate is calculated to be 2.58%. This method effectively assesses whether numerical values such as contact depth meet the required standards, thereby mitigating potential issues.

Additionally, mesh reconstruction and texture mapping are employed to ensure the proper connection and appearance of the turnout machine. As depicted in Figure 6, the texture-mapped model of the turnout machine is displayed. For further visual comparison, Figure 10 presents close-up shots of partial images from the captured dataset, while Figure 11 shows close-up shots of the three-dimensional model after texture mapping. A comparison between the two reveals that the three-dimensional model after texture mapping accurately reconstructs the three-dimensional scene of the turnout machine, facilitating better monitoring of its status.



Figure 10. Partial image of image data set



Figure 11. Partial close-up of the texture map model

## 5. Conclusion

This paper proposes an image-based detection method for railway turnout machines. Leveraging multiple images and three-dimensional reconstruction algorithms, it achieves the reconstruction of three-dimensional models of railway turnout machines. By analyzing point cloud information, it assesses whether issues such as the dynamic-static contact point status and appearance of the railway turnout machine comply with detection standards, thereby reducing the workload of maintenance personnel in conducting inspections. Moreover, by retaining data for future reference, it provides crucial evidence for subsequent reviews, effectively enhancing operational efficiency. With the increasing sophistication of intelligent systems and the advancement of computing power in future work, algorithms can be further enhanced to include gap inspections of turnout machines, enabling integrated detection. Furthermore, real-time uploading and analysis via networked platforms can expedite the detection process and enhance operational reliability.

## References

- [1] DU Tongtong. Review on Gap Detection Methods of Switch Machine [J]. Modern Manufacturing Technology and Equipment, 2022, 58(02):162-164.
- [2] ZHANG Yifan, CHENG Yifei, CHEN Hongxia. Research on notch monitoring system of switch machine [J]. Technology Innovation and Application, 2021, 11(22):44-46.
- [3] HE Hui, DAI Meng, LI Xue, TAO Weijie. Research on Intelligent Fault Diagnosis Method for Turnouts Based on DCNN-SVM [J]. Journal of the China Railway Society, 2023, 45(09):103-113.

- [4] DU Sen, ZHANG Shou, LIANG Jingyuan, LIU Songhe. Switch Machine Gap Edge Detection Algorithm Based on Pixel Quantity Count[J]. Urban Mass Transit, 2023, 26(07):241-245.
- [5] LIU Yunting, CHEN Guangwu. Automatic detection of switch machine gap based on SFFCM image segmentation [J]. Journal of Beijing Jiaotong University, 2022, 46(02):29-36.
- [6] SHI cong. Movable/Static Contact State Detection Technology of Metro Turnout Switch Machine Based on Image Processing [J]. Urban Mass Transit, 2020, 23(S2):149-152.
- [7] HU xiaoxi, CAO Yuan, TANG Tao. Measurement of Stationary Contacts of Switch Circuit Controller in Point Machines Based on Deep Convolutional Feature Matching [J]. Journal of the China Railway Society, 2023, 45(05):57-64.
- [8] Furukawa Y, Hernández C. Multi-view stereo: A tutorial[J]. Foundations and Trends® in Computer Graphics and Vision, 2015, 9(1-2): 1-148.
- [9] Schonberger J L, Frahm J M. Structure-from-motion revisited[C]//Proceedings of the IEEE Conference on Computer Vision and Pattern Recognition. 2016: 4104-4113.
- [10] Snavely N, Seitz S M, Szeliski R. Modeling the world from internet photo collections[J]. International Journal of Computer Vision, 2008, 80: 189-210.